Article

Cell Metabolism

Oxygen and Carbon Dioxide Rhythms Are Circadian Clock Controlled and Differentially Directed by Behavioral Signals

Graphical Abstract

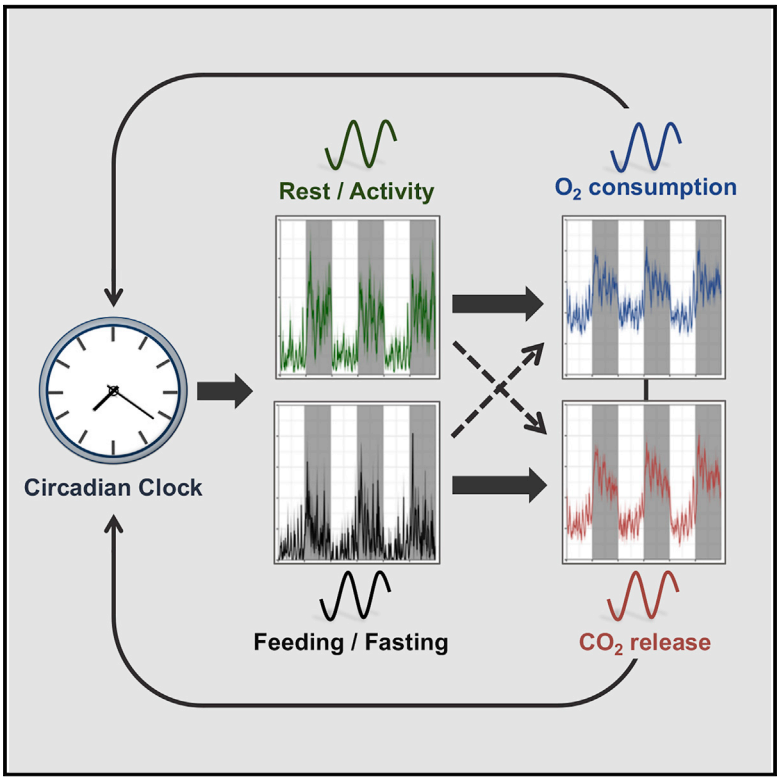

Authors

Yaarit Adamovich, Benjamin Ladeuix, Jonathan Sobel, ..., Ariel Tarasiuk, Maarten P. Koeners, Gad Asher

Correspondence

gad.asher@weizmann.ac.il

In Brief

Adamovich et al. show that the daily regulation of oxygen consumption and carbon dioxide release is regulated by the circadian clock. Time-restricted feeding restores oxygen and carbon dioxide rhythms in clock mutants. Their findings also support a potential role for carbon dioxide in phase resetting of peripheral clocks upon feeding

Highlights

- Circadian clocks control daily oxygen and carbon dioxide rhythms
- Time-restricted feeding restores oxygen and carbon dioxide rhythms in clock mutants
- Day-time feeding dissociates oxygen cycles from carbon dioxide rhythms
- Carbon dioxide levels affect the core clock gene expression and phase shift the clock

Adamovich et al., 2019, Cell Metabolism *29*, 1092–1103
May 7, 2019
https://doi.org/10.1016/j.cmet.2019.01.007

CellPress

Oxygen and Carbon Dioxide Rhythms Are Circadian Clock Controlled and Differentially Directed by Behavioral Signals

Yaarit Adamovich,[1,6] Benjamin Ladeuix,[1,6] Jonathan Sobel,[1] Gal Manella,[1] Adi Neufeld-Cohen,[1] Mohammad H. Assadi,[3] Marina Golik,[1] Yael Kuperman,[4] Ariel Tarasiuk,[2,3] Maarten P. Koeners,[5] and Gad Asher[1,7,*]

[1]Department of Biomolecular Sciences, Weizmann Institute of Science, Rehovot 7610001, Israel
[2]Sleep-Wake Disorders Unit, Soroka University Medical Center, Faculty of Health Sciences, Ben-Gurion University of the Negev, Beer-Sheva, Israel
[3]Department of Physiology and Cell Biology, Faculty of Health Sciences, Ben-Gurion University of the Negev, Beer-Sheva, Israel
[4]Department of Veterinary Resources, Weizmann Institute of Science, Rehovot 7610001, Israel
[5]Institute of Biomedical and Clinical Science, University of Exeter Medical School, University of Exeter, Exeter, UK
[6]These authors contributed equally
[7]Lead Contact
*Correspondence: gad.asher@weizmann.ac.il
https://doi.org/10.1016/j.cmet.2019.01.007

SUMMARY

Daily rhythms in animal physiology are driven by endogenous circadian clocks in part through rest-activity and feeding-fasting cycles. Here, we examined principles that govern daily respiration. We monitored oxygen consumption and carbon dioxide release, as well as tissue oxygenation in freely moving animals to specifically dissect the role of circadian clocks and feeding time on daily respiration. We found that daily rhythms in oxygen and carbon dioxide are clock controlled and that time-restricted feeding restores their rhythmicity in clock-deficient mice. Remarkably, day-time feeding dissociated oxygen rhythms from carbon dioxide oscillations, whereby oxygen followed activity, and carbon dioxide was shifted and aligned with food intake. In addition, changes in carbon dioxide levels altered clock gene expression and phase shifted the clock. Collectively, our findings indicate that oxygen and carbon dioxide rhythms are clock controlled and feeding regulated and support a potential role for carbon dioxide in phase resetting peripheral clocks upon feeding.

INTRODUCTION

The prevalence of daily rhythms in almost every aspect of biology in mammals has been a subject of intensive research in the past years. Among others, these include characterization of daily oscillations in gene expression, protein and metabolite accumulation, and overt rhythms in physiology (e.g., core body temperature, heart rate, and blood pressure) and behavior (e.g., activity and feeding) (Asher and Sassone-Corsi, 2015; Bass and Lazar, 2016; Curtis and Fitzgerald, 2006; Panda, 2016). These rhythms are governed by endogenous cell autonomous oscillators in conjunction with external inputs such as light-dark cycles that modulate rest-activity and consequently feeding behavior (Dibner et al., 2010; Partch et al., 2014; Takahashi, 2017). The intricate interplay between endogenous rhythms and environmental cues in control of various rhythmic outputs plays a critical role in animal homeostasis. The dissection of these components in the context of whole-animal physiology, which readily responds to external inputs and relies as well on endogenous rhythms, is of great interest.

A vital element in a mammals' physiology is respiration, namely, the exchange of oxygen from the outside environment into cells within tissues in return for carbon dioxide transport in the opposite direction. In cells, the mitochondria use nutrients such as carbohydrates and lipids and convert them to energy coins upon oxygen consumption and carbon dioxide release. Oxygen is primarily consumed in mitochondria through oxidative phosphorylation, whereas carbon dioxide is the product of the citric acid cycle (Akram, 2014; Wilson et al., 1988).

This fundamental process exhibits daily rhythms, as pulmonary ventilation normally rises during the active phase and drops during the resting phase (Mortola, 2004). Consequently, the oxygen consumption rate, as well as blood and tissue oxygenation, in mammals exhibits daily oscillations (Adamovich et al., 2017; Emans et al., 2017). We recently reported that oxygen rhythms within the physiological range synchronize circadian clocks in a Hypoxia Inducible Factor 1 alpha (HIF1α)-dependent manner and that modulation of ambient oxygen levels accelerates jet-lag adaptation (Adamovich et al., 2017). Bass and colleagues further demonstrated that HIF1α regulates the circadian period and that circadian clock disruption impairs oxygen sensing through HIF1α (Peek et al., 2017). Furthermore, an interplay between the DNA-binding activity of HIF1α and the core clock protein BMAL1 as well as physical interaction was reported (Hogenesch et al., 1998; Wu et al., 2017). Collectively, these studies point toward an intricate interplay between oxygen rhythmicity and circadian clock control. Understanding the principles underlying daily oscillations in oxygen levels are, therefore, of great interest. Furthermore, since oxygen is exchanged with carbon dioxide during respiration, this raises

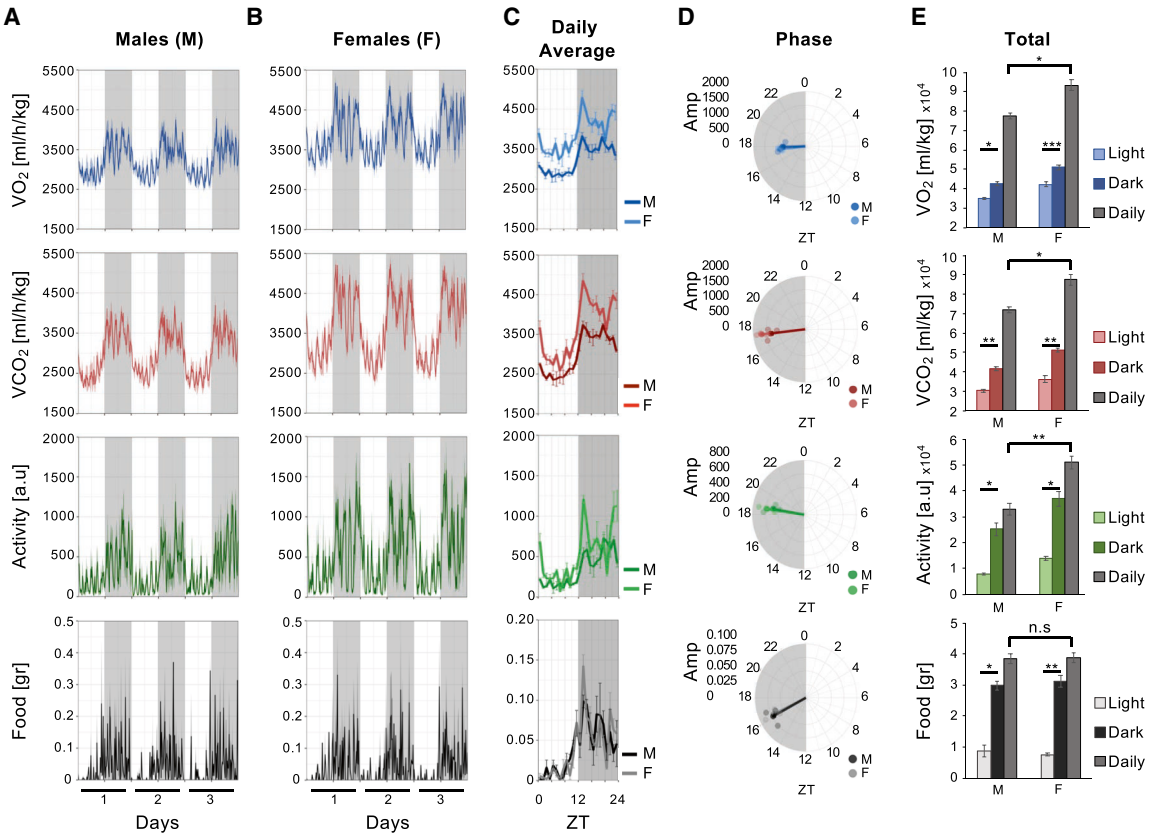

Figure 1. Daily Rhythms in Oxygen Consumption and Carbon Dioxide Release

Wild-type male (A) and female (B) mice were housed under 12 h light-dark cycles. Metabolic cages were used to monitor oxygen consumption rate (VO_2) (blue), carbon dioxide release rate (VCO_2) (red), spontaneous locomotor activity (green), and food intake (black). Data are presented as the mean ± SEM of 3 mice, recorded at 15 min intervals for 3 consecutive days, alongside the mean ± SEM of 3 days' average of each individual mouse (C), the calculated phase and amplitude (Amp) based on 24 h cosine fit analysis (D), and the total (mean ± SEM) for the light phase, dark phase, and the entire day. (E). ZT, Zeitgeber time; gray shadings represent the dark phases. t test, *p < 0.05, **p < 0.01, and ***p < 0.001.

See also Figure S1.

the question regarding the profile and determinants of carbon dioxide release throughout the day.

In the current study, we employed metabolic cages to measure oxygen consumption, carbon dioxide release, food intake, and locomotor activity alongside a telemetric system to record tissue (e.g., kidney) oxygenation in freely moving animals and dissected the daily control of oxygen and carbon dioxide by circadian clocks, light-dark cycles, and feeding rhythms. Specifically, we asked the following questions: (1) What regulates the daily oscillations in oxygen consumption and tissue oxygenation; (2) are there daily rhythms in carbon dioxide release and what controls them? (3) Can these processes be disintegrated and what are the potential molecular downstream effects? We found that daily rhythms in oxygen and carbon dioxide are under circadian clock control and feeding. Importantly, day-time feeding dissociated oxygen rhythms from carbon dioxide oscillations, whereby the former followed activity and the latter was shifted and aligned with food intake. Finally, we demonstrated that changes in carbon dioxide levels, at least in cultured cells, alter clock-gene expression and phase shift the clock, thus supporting a potential role of carbon dioxide in phase resetting of circadian clocks in peripheral organs *in vivo*.

RESULTS

Daily Rhythms in Oxygen Consumption, Tissue Oxygenation, and Carbon Dioxide Release

We monitored daily changes in respiration (i.e., oxygen consumption and carbon dioxide release) as well as spontaneous locomotor activity and food intake of freely moving male and female mice at high temporal resolution using metabolic cages (Figure 1). As expected from nocturnal animals, locomotor activity and food consumption were elevated during the dark phase and were accompanied by an increase in oxygen consumption. The rise in oxygen consumption during the dark phase was associated with an increase in carbon dioxide release, which exhibited a similar daily profile as oxygen consumption (Figures 1A–1C). A cosine fit with a 24 h period assigned similar phases (Zeitgeber time [ZT] ~18) for the 4 parameters, namely oxygen consumption and carbon dioxide release, locomotor activity, and food intake, for both males and females (Figure 1D). Notably, females showed elevated respiration compared to males with higher total oxygen consumption and carbon dioxide release (Figures 1C and 1E). This is consistent with the fact that smaller animals (e.g., female compared to male mice) have higher

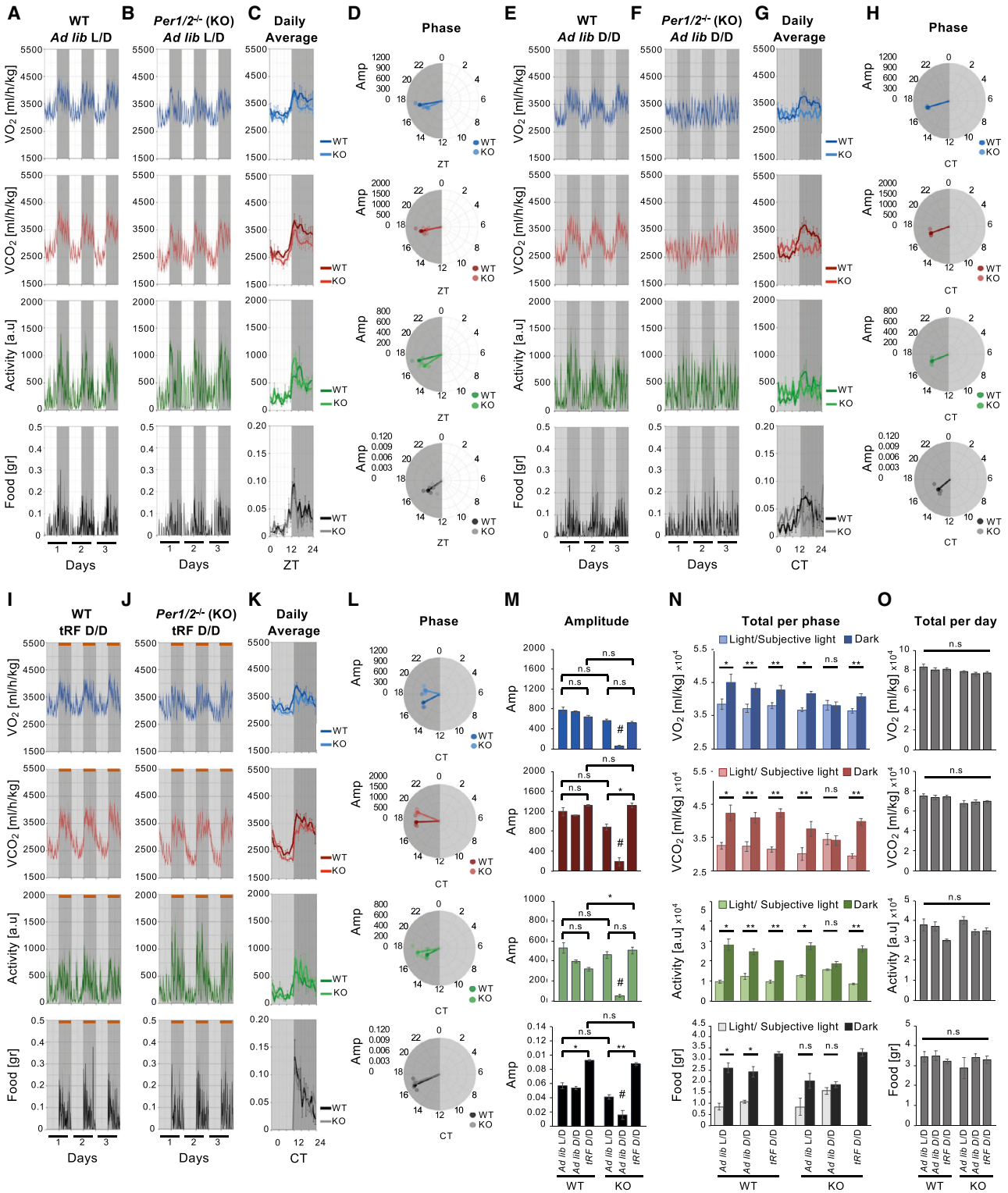

Figure 2. Time-Restricted Feeding Restores Daily Oxygen and Carbon Dioxide Rhythms in *Per1/2*$^{-/-}$ Mice in Dark-Dark

Wild-type (WT) and *Per1/2*$^{-/-}$ (KO) mice were housed under a 12 h light-dark regimen (A–D) or dark-dark regimen (E–L) and fed either *ad libitum* (*Ad lib*) (A–H) or exclusively during the subjective night (tRF) (I–L). The same cohort of mice was used for all conditions. Metabolic cages were used to monitor oxygen consumption rate (VO_2) (blue), carbon dioxide release rate (VCO_2) (red), spontaneous locomotor activity (green), and food consumption (black). Data are presented as the mean ± SEM of 3 mice, recorded at 15 min intervals for 3 consecutive days (A, B, E, F, I, and J), alongside the mean ± SEM of 3 days' average of each individual mouse (C, G, and K), the calculated phase (D, H, and L) and amplitude (mean ± SEM) based on 24 h cosine fit analysis (M), the total (mean ± SEM) for the Light and

(legend continued on next page)

energy expenditure (Schmidt-Nielsen, 1983), which might be in part due to their elevated locomotor activity (Figure 1E). Likewise, metabolic cage analyses of male rats revealed similar daily rhythms in the above-indicated parameters (Figures S1A–S1D). Overall, these findings are in line with previous measurements of indirect calorimetry in rodents (Fischer et al., 2018; Meyer et al., 2015; Tschöp et al., 2011).

Continuous recordings of tissue oxygenation (i.e., kidney and liver) from freely moving rats using a telemetric oxygen monitoring system (Figure S1E) evinced overt daily rhythms in line with our metabolic cage analyses and in agreement with the previous work of others and our own (Adamovich et al., 2017; Emans et al., 2017). Remarkably, the whole animal profile of oxygen consumption was relatively square shaped (Figures 1A–1C and S1A–S1B), while kidney and liver oxygen profiles exhibited more of a sine waveform (Figure S1E), signifying the presence of homeostatic mechanisms that mitigate the sharp changes in oxygen consumption between the resting and active phases. Of note, because of the size and weight of the oxygen sensor, telemetric oxygen measurements are currently non-feasible in mice and were therefore limited to experiments with rats.

The presence of overt rhythms in oxygen consumption, tissue oxygenation, and carbon dioxide release in animals fed *ad libitum* prompted us to examine potential determinants that drive and coordinate these rhythms.

Circadian Clocks Control Daily Rhythms in Oxygen Consumption and Carbon Dioxide Release

As aforementioned, circadian clocks are implicated in daily regulation of physiology and behavior in mammals. At the cellular level, clocks control daily rhythms in mitochondrial respiration (Manella and Asher, 2016; Neufeld-Cohen et al., 2016; Peek et al., 2013). We, therefore, examined the role of circadian clocks in control of daily oxygen consumption and carbon dioxide release. To this end, we employed two different clock mutant mouse models, namely Bmal1$^{-/-}$ and *Per1/2*$^{-/-}$ mice. In the former, the positive (activator) limb of the core clock oscillator is compromised, and in the latter, the negative (repressor) arm is impaired. Both clock mutant mouse models exhibit arrhythmic locomotor activity in constant dark, and circadian expression of core clock and clock-controlled genes is largely diminished (Adamovich et al., 2014; Bunger et al., 2000; Zheng et al., 2001).

Overall, under a 12 h light-dark regimen, both PER1/2-deficient and BMAL1-deficient animals preserved the daily rhythmicity in oxygen consumption and carbon dioxide release (Figures 2A–2C and S2A–S2C for *Per1/2*$^{-/-}$ and *Bmal1*$^{-/-}$, respectively) with similar phases (Figures 2D and S2D), yet the amplitude was reduced exclusively in the case of BMAL1-deficient mice (Figures 2M and S2M). Interestingly, the oxygen and carbon dioxide profiles of PER1/2 null mice mostly differed from their wild-type counterparts during the dark phase, whereas a greater difference was observed in the case of BMAL1-deficient mice in the light phase (Figures 2C and S2C). This was evident as well in the oxygen and carbon dioxide levels in the day versus night comparison (Figures 2N and S2N).

As expected and in contrast to wild-type mice, both PER1/2-deficient and BMAL1-deficient mice showed no rhythmicity in locomotor activity, as well as feeding behavior, in constant dark. Notably, oxygen consumption and carbon dioxide release were relatively constant throughout the day in both clock mutant mouse models (Figures 2E–2G and S2E–S2G for *Per1/2*$^{-/-}$ and Bmal1$^{-/-}$, respectively). In accordance, the amplitude of the 24 h cosine fit was lower than the standard deviation of the data for both PER1/2-deficient and BMAL1-deficient mice; therefore, it was considered non-rhythmic and a phase was not assigned (Figures 2H and 2M for *Per1/2*$^{-/-}$ and Figures S2H and S2M for Bmal1$^{-/-}$).

Based on the above-described experiments conducted with two different clock deficient mouse models, we concluded that oxygen and carbon dioxide rhythms are circadian clock controlled, plausibly through driving rhythmic activity and feeding behavior.

Time-Restricted Feeding Restores Daily Oxygen and Carbon Dioxide Rhythms in the Absence of a Functional Clock

To test the specific role of cyclic feeding behavior in driving rhythms in oxygen consumption and carbon dioxide release, we imposed time-restricted feeding during the subjective night on PER1/2-deficient and BMAL1-deficient mice housed in constant dark. Overall, time-restricted feeding restored rhythmicity in oxygen consumption and carbon dioxide release with similar phases as in wild-type mice in both clock mutant mouse models (Figures 2I–2L and S2I–S2L for *Per1/2*$^{-/-}$ and Bmal1$^{-/-}$, respectively). Here again, the amplitude was shallower in BMAL1-deficient compared to PER1/2-deficient and wild-type mice (Figures 2M and S2M).

Next, we examined the potency of light-dark versus feeding-fasting cycles as drivers of daily rhythms in oxygen consumption and carbon dioxide release in the absence of a functional clock. Our analysis evinced that in both clock mutant mouse models, namely PER1/2-deficient and BMAL1- deficient mice, the effects of light-dark cycles and feeding-fasting rhythms are comparable. Both Zeitgebers restored rhythmicity in oxygen consumption and carbon dioxide release with similar phases and amplitudes (Figures 2L–2M and S2L–S2M). Yet, we noted a trend toward higher amplitude in carbon dioxide rhythms upon time-restricted feeding compared to light-dark cycles irrespective of the clock mutant mouse model tested. Overall, we did not observe any significant changes in total oxygen consumption, carbon dioxide release, activity, or food consumption throughout the day between the different mouse strains regardless of the light or feeding regimen tested above (Figures 2O and S2O).

Taken together, our findings indicate that daily oscillations in oxygen and carbon dioxide are under circadian clock control and that feeding rhythms are sufficient to drive their rhythmicity

Dark phases (N), and the total per day (mean ± SEM) (O). For (A)–(D), gray shadings represent the dark phases. For (E)–(L), dark and light gray shadings represent the subjective dark and light phases, respectively. ZT, Zeitgeber time; CT, circadian time; L/D, 12 h light-dark; D/D, constant dark. Orange bars mark times of food availability. t test, *p < 0.05, **p < 0.01, n.s, non-specific. # marks cases in which amplitude divided by the S.D. of the data was below 1, hence considered not to exhibit 24 h rhythmicity.

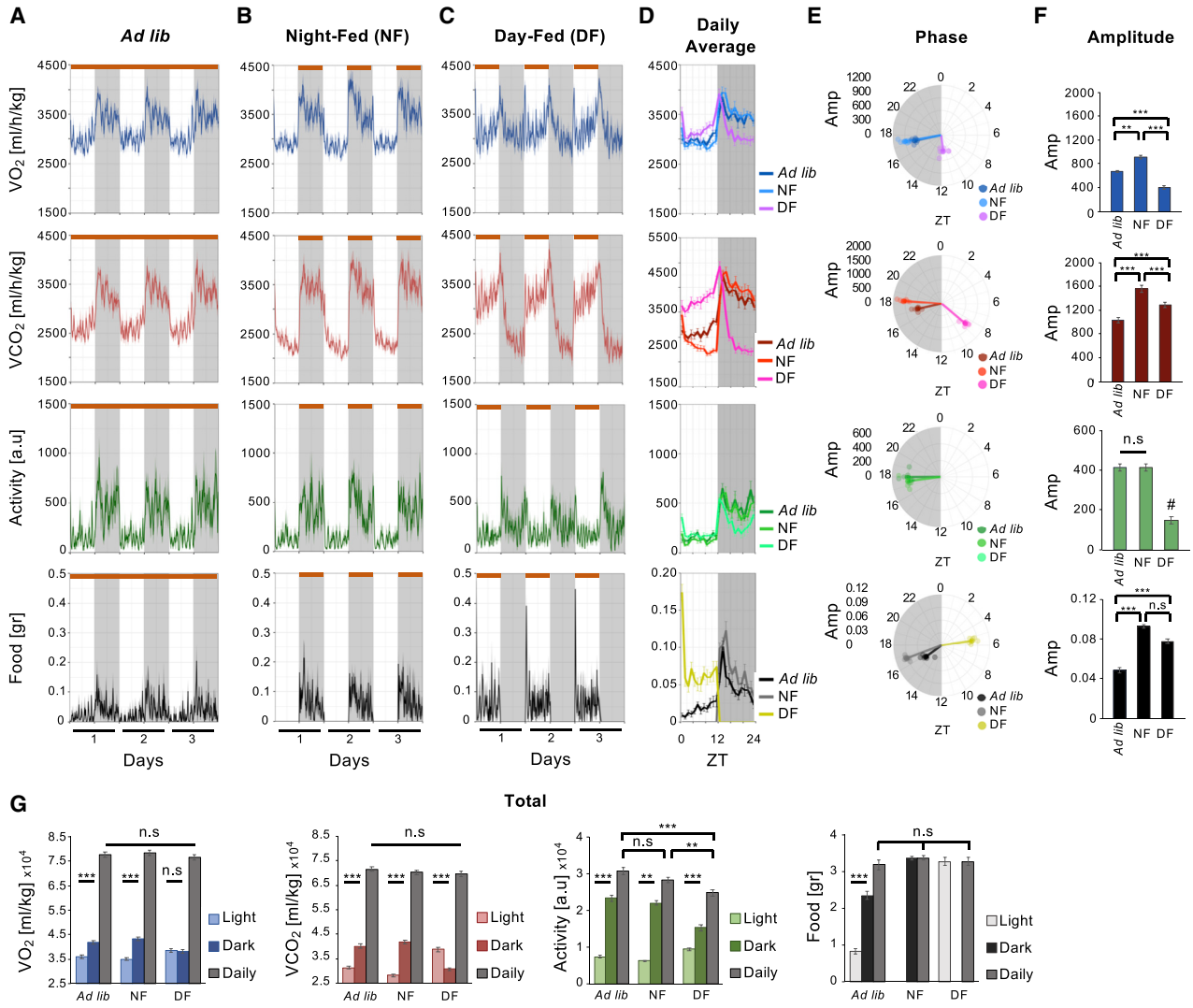

Figure 3. The Effect of Feeding Time on Daily Oxygen and Carbon Dioxide Rhythms in Wild-type Mice

Wild-type mice were housed under a 12 h light-dark regimen and either fed *ad libitum* (*Ad-lib*) (A), during the dark phase (days 2–4 upon night-feeding), (night-fed [NF]) (B), or during the light phase (days 3–5 upon day-feeding), (day-fed [DF]) (C). The same cohort of mice was used for all 3 conditions. Metabolic cages were used to monitor oxygen consumption rate (VO_2) (blue), carbon dioxide release rate (VCO_2) (red), spontaneous locomotor activity (green), and food consumption (black). Data are presented as the mean of 7 mice, recorded at 15 min intervals for 3 consecutive days, (A–C) alongside the mean ± SEM of 3 days' average of each individual mouse (D), the calculated phase (E), the amplitude (mean ± SEM) based on 24 h cosine fit analysis (F), and the total (mean ± SEM) for the light phase, dark phase, and the entire day (G). ZT, Zeitgeber time; n.s, non-specific; gray shadings represent the dark phases. Orange bars mark times of food availability. t test, $^{**}p < 0.01$, $^{***}p < 0.001$.

marks cases in which amplitude divided by the S.D. of the data was below 1, hence considered not to exhibit 24 h rhythmicity. See also Figure S3.

independently of the clock. Since the cyclic feeding behavior carried a more pronounced effect on carbon dioxide rhythms than on oxygen oscillations in both clock mutant mouse models, we posited that carbon dioxide rhythms might be dominated by feeding behavior.

Feeding Time Alters Daily Rhythms in Oxygen Consumption, Tissue Oxygenation, and Carbon Dioxide Release

To delineate the specific role of feeding schedule on oxygen and carbon dioxide rhythms, wild-type animals were fed either exclusively during the dark (night-fed) or during the light phase (day-fed). Similar to animals fed *ad libitum*, night-fed animals exhibited robust daily rhythms in oxygen consumption and carbon dioxide release (Figures 3A, 3B, and 3D), with comparable phases (Figure 3E) yet higher amplitude in night-fed animals (Figure 3F). Notably, in night-fed animals, the night-day ratio in oxygen consumption was slightly elevated compared to mice fed *ad libitum* (from 1.17 in *ad libitum* to 1.24 in night-fed), whereas a more pronounced effect was observed for carbon dioxide (from 1.28 in *ad libitum* to 1.48 in night-fed) (Figure 3G), thus further supporting the prominent effect of feeding on carbon dioxide. The total daily oxygen consumption and carbon dioxide release were similar under both feeding regimens (Figure 3G).

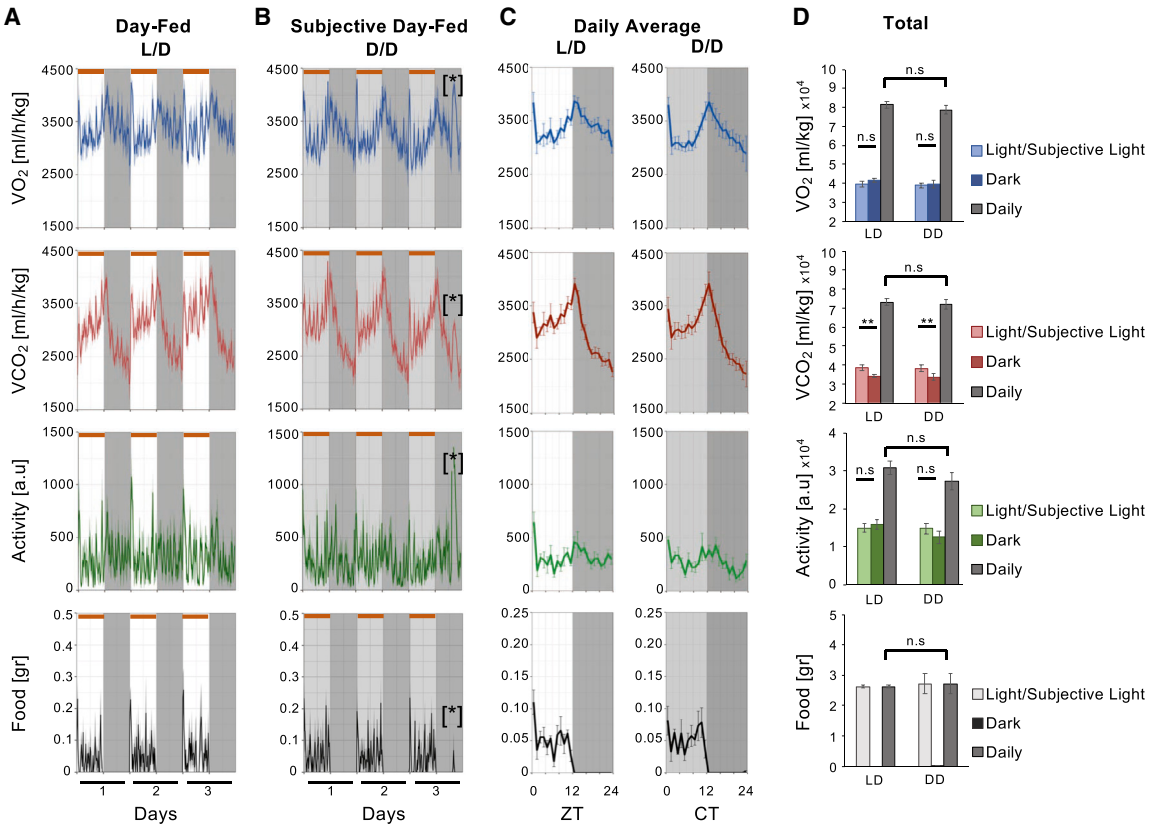

Figure 4. The Effect of Feeding Time on Daily Oxygen and Carbon Dioxide Rhythms is Light-Dark Cycle Independent

(A and B) Wild-type mice were housed under a 12 h light-dark (L/D) (A), or Dark-Dark (D/D) (B) and fed exclusively during the light phase (subjective light phase in D/D). The same cohort of mice was used for both conditions. Metabolic cages were used to monitor oxygen consumption rate (VO_2) (blue), carbon dioxide release rate (VCO_2) (red), spontaneous locomotor activity (green), and food consumption (black). Data are presented as the mean of 5 mice, recorded at 15-min intervals for 3 consecutive days, (A and B), alongside the mean ± SEM of 3 days' average of each individual mouse for the L/D condition and the mean ± SEM of two days' average of each individual mouse for the D/D condition (due to a technical problem marked with [*]) (C), and the total (mean ± SEM) for the light phase, dark phase and the entire day (D). ZT, Zeitgeber time; CT, circadian time. For (A), gray shadings represent the dark phases. For (B), dark and light gray shadings represent the subjective dark and light phases, respectively. Orange bars mark times of food availability. t test, **p < 0.01, n.s, non-specific.
[*] marks a transient technical problem in the recordings (automated feeders were open for 2 h at the wrong time).

By contrast, day-time feeding resulted in pronounced effects on the daily profiles of oxygen, carbon dioxide, and locomotor activity in comparison to night-time or *ad libitum* feeding. First, instead of a single peak in night-time or *ad libitum* feeding, we now observed two peaks, both for oxygen consumption and locomotor activity, one in the beginning of the light phase and a second peak at the interphase between the light and dark phases (Figures 3C and 3D). Consistently, a 24 h cosine fit that was used to compute the phase and amplitude was either lower than (locomotor activity) or very close to (oxygen consumption) the standard deviation of the data (Figure 3F). Therefore, in the absence of a reliable cosine fit, we refrained from plotting the computed phase in Figure 3E and thereafter (i.e., Figures 4, 5, S3, and S4). Second, the total oxygen consumption during the day-time and night-time was even (Figure 3G). Third, the daily profile of carbon dioxide largely differed from the one detected for oxygen and locomotion. We did not observe two distinct peaks for carbon dioxide release but rather a complete inversion with elevated levels during the light phase compared to the night phase in accord with feeding time (Figures 3C, 3D, and 3G). The effect of day-time feeding on oxygen consumption and carbon dioxide release was preserved in female mice (Figures S3A–S3D), suggesting that the phenomenon is gender independent. Furthermore, the additional sharp peak in oxygen consumption upon day-time feeding at the beginning of the light phase was evident as well in kidney oxygenation as measured in freely moving rats using our telemetric tissue oxygen monitoring system (Figure S3E).

Taken together, our results suggest that feeding schedule shapes the daily profiles of oxygen consumption and tissue oxygenation, as well as carbon dioxide release. Remarkably, day-time feeding dissociated oxygen rhythms from carbon dioxide oscillations, whereby oxygen rhythms followed locomotor activity and carbon dioxide oscillations were shifted and aligned with food intake.

The Effects of Day-Time Feeding on Oxygen and Carbon Dioxide Rhythms Are Light Independent and Do Not Require a Functional Molecular Clock

The striking differential effect of day-time feeding on oxygen and carbon dioxide rhythms prompted us to examine potential

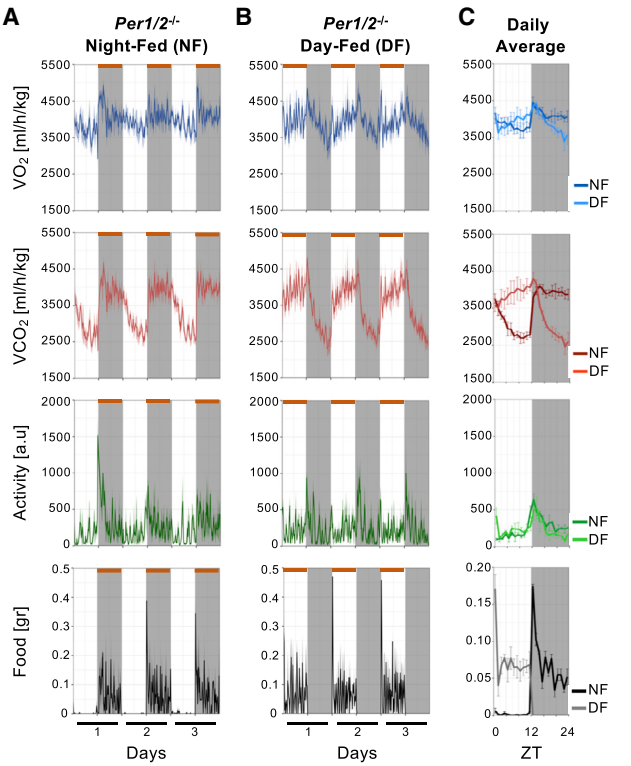

Figure 5. The Effect of Feeding Time on Daily Oxygen and Carbon Dioxide Rhythms in *Per1/2*$^{-/-}$ Mice

(A and B) *Per1/2*$^{-/-}$ mice were housed under a 12 h light-dark regimen and fed exclusively during the dark phase (days 2–4 upon night-feeding) (A) or fed exclusively during the light phase (days 3–5 upon day-feeding), (D/F) (B). The same cohort of mice was used for both conditions. Metabolic cages were used to monitor oxygen consumption rate (VO_2) (blue), carbon dioxide release rate (VCO_2) (red), spontaneous locomotor activity (green), and food consumption (black). Data are presented as the mean of 3 mice, recorded at 15 min intervals for 3 consecutive days (A and B) alongside the mean ± SEM of 3 days' average of each individual mouse (C), and the total (mean ± SEM) for the light phase, dark phase, and the entire day (D). ZT, Zeitgeber time; n.s, non-specific; gray shadings represent the dark phases. Orange bars mark times of food availability. t test, *p < 0.05, ***p < 0.001. See also Figure S4.

underlying determinants, namely light-dark and the molecular clock. Since light carries a dominant effect on rodents' behavior, and mice normally limit their locomotor activity to the dark and minimize it during the light phase, we first asked whether light plays a role in the observed pattern of oxygen and carbon dioxide rhythms upon day-time feeding. Wild-type mice were housed either under a 12 h light-dark regimen or in constant dark and fed exclusively during the light phase or in the subjective light phase in the case of constant dark (Figure 4). The two peaks in oxygen consumption and activity and the inversion in carbon dioxide release were preserved in constant dark, and their profiles resembled to mice housed under the light-dark regimen (Figures 4A–4D).

Next, we asked whether these effects are dependent on the molecular clock. To this aim, we employed the *Per1/2*$^{-/-}$ and Bmal1$^{-/-}$ clock mutant mice and fed them either exclusively during the dark or the light phase (Figures 5A–5D and S4A–S4D for *Per1/2*$^{-/-}$ and Bmal1$^{-/-}$, respectively). Similar to wild-type mice (Figures 3 and 4) and in contrast to night-fed animals, PER1/2-deficient and BMAL1-deficient mice exhibited two peaks in oxygen consumption and locomotor activity and an inversion in carbon dioxide release upon day-time feeding.

We concluded that the effects of day-time feeding on oxygen and carbon dioxide rhythms are light-independent and do not require a functional molecular clock.

The Effects of Day-Time Feeding on Oxygen and Carbon Dioxide Rhythms Are Immediate and Sustained

Hitherto, we identified a prominent effect of day-time feeding on oxygen and carbon dioxide rhythms during days 3 to 5 of day-time feeding (Figures 3, 4, 5, S3, and S4). Previous studies that addressed the effect of day-time feeding on circadian clock gene expression evinced that day-time feeding uncouples peripheral clocks (e.g., liver, kidney) from the master clock in the SCN region of the brain and that this effect is gradual and takes about a week to be completed (Asher et al., 2010; Damiola et al., 2000; Mukherji et al., 2015; Saini et al., 2013; Stokkan et al., 2001). Hence, it raised the intriguing question whether the observed alterations in oxygen and carbon dioxide rhythms are the direct consequence of changes in feeding, that in turn modulate rhythmic gene expression in peripheral tissues or vice versa, namely feeding alters rhythmic gene expression and consequently affects daily respiration. To address this chicken-and-egg question, we set out to perform a kinetic experiment in which mice were continually monitored in metabolic cages for 16 consecutive days. In the first 3 days, mice were night-fed. Then, on day 4, food was impeded, and subsequently, the mice were shifted to day-time feeding for 9 days. Finally, food was provided *ad libitum* for 3 days (Figure 6). Notably, during the 24 h of food deprivation, carbon dioxide release, in contrast to oxygen consumption, did not reach the same level as in night-fed animals but rather gradually dropped (Figure S5A), consistent with the prominent effect of food intake on carbon dioxide levels.

Upon 8 days of day-time feeding, we observed a complete inversion of circadian clock gene expression in the liver, in agreement with previous reports (Asher et al., 2010; Damiola et al., 2000; Mukherji et al., 2015), (Figure S5B). Our analyses showed that the two peaks in oxygen consumption and spontaneous activity, as well as the shift in carbon dioxide release, appear already from the first day of day-time feeding (Figure 6A) and are preserved for 9 consecutive days with similar peak times (Figure 6B) and day versus night levels (Figure 6C). Likewise, once mice are shifted back from day-feeding to *ad libitum*, the response is immediate. Hence, we concluded that the phenomenon is not transient, but rather sustained, and that it appears

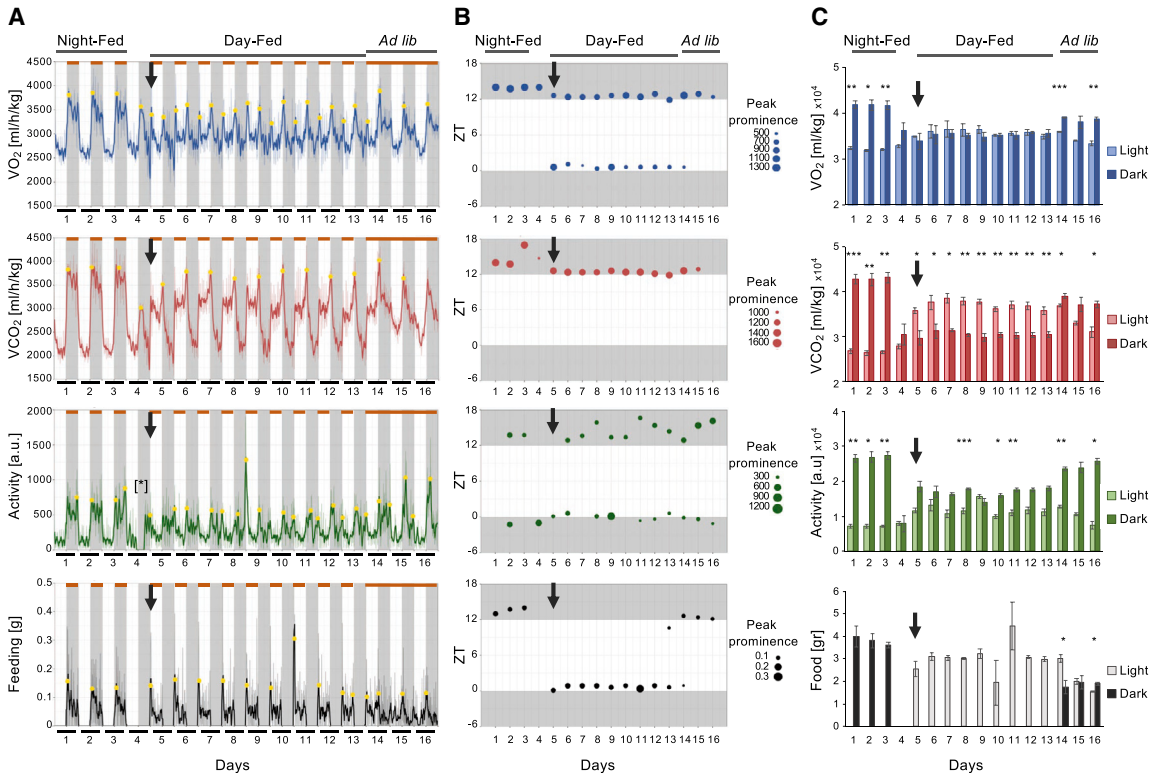

Figure 6. The Effects of Day-Time Feeding on Oxygen and Carbon Dioxide Rhythms Are Immediate and Sustained

Wild-type mice were continually monitored in metabolic cages for 16 consecutive days; in the first 3 days, mice were night fed; then on day 4, food was impeded; subsequently, mice were shifted to day-time feeding for 9 days; next, food was provided *ad libitum* for 3 days.

Metabolic cages were used to monitor oxygen consumption rate (VO_2) (blue), carbon dioxide release rate (VCO_2) (red), spontaneous locomotor activity (green), and food consumption (black). Data are presented as the mean of 3 mice, recorded at 15 min intervals for 3 consecutive days (A), alongside the peak detection in each day (the last peak in VCO_2 data was not detected due to edge effect) (B), and the total (mean ± SEM) for the Light phase and Dark phase for each day (C). ZT, Zeitgeber time; n.s, non-specific; gray shadings represent the dark phase. The circle size represents the prominence of the peak. The arrow indicates the first day of day-time feeding. Orange bars mark times of food availability. t test, *p < 0.05, ** p < 0.01 ***p < 0.001. [*] marks an unexpected technical problem in the activity recordings for 9 h (another set of recordings for the 24 h of food deprivation is presented in Figure S5A). See also Figure S5.

instantly upon day-time feeding. It is, therefore, conceivable that the observed changes in respiration upon day-time feeding are upstream to the gradual changes in circadian clock gene expression in peripheral tissues and might even play a role in this process.

Carbon Dioxide Levels Affect Core Clock Gene Expression and Phase Shift the Clock

The sustained and immediate effect of day-time feeding on respiration, in particular the prominent and rapid inversion of carbon dioxide rhythms in alignment with feeding time, prompted us to examine whether carbon dioxide levels affect core clock gene expression and consequently phase shift the clock.

To this end, we employed cell culture assays in which carbon dioxide levels can be well controlled. We first tested the effect of lowering carbon dioxide levels on the expression of the core clock genes (Figure 7A). Time course analysis revealed that moving from standard growth conditions of 5% carbon dioxide to 1% affect the expression of several core clock genes in cultured cells, in particular *Rev-Erb* α, *Per2*, *Cry1*, and *Dbp*. Interestingly, the transcript levels of both *Per2* and *Cry1* were up-regulated, whereas *Rev-Erb* α and *Dbp* were down-regulated. *Clock*, *Bmal1*, as well as *Per1* and *Cry2* were relatively unaffected. The effect of carbon dioxide on core clock gene expression encouraged us to test whether these changes are sufficient to elicit a phase shift. To this aim, we used the NIH3T3 cell line that stably expresses a luciferase reporter gene under the control of the *Bmal1* promoter (*Bmal1*-luciferase reporter) (Nagoshi et al., 2004). A shift from 5% to 1% resulted in a phase advance of almost 5 h (Figure 7B). Notably, a pulse of 10 h of 1% carbon dioxide had a more pronounced effect with a phase shift of ~8 h (Figure 7C).

This differential effect incited us to perform a phase response curve (PRC). The PRC illustrates the relationship between time of administration (relative to the internal circadian clock) and the magnitude of the treatment's effect on circadian phase. Hence, we exposed the cells to a 2 h pulse of low carbon dioxide (i.e., 1%) during different time points within the circadian cycle and analyzed the phase shift based on the bioluminescence recording of the NIH3T3:*Bmal1*-luciferase cells (Figure S6). Based on the data depicted in Figure S5, we generated a PRC, in which the magnitude of the phase shift was plotted against circadian time (Figure 7D). Our PRC evinced that the magnitude and the direction of the phase shift depends on the time of the

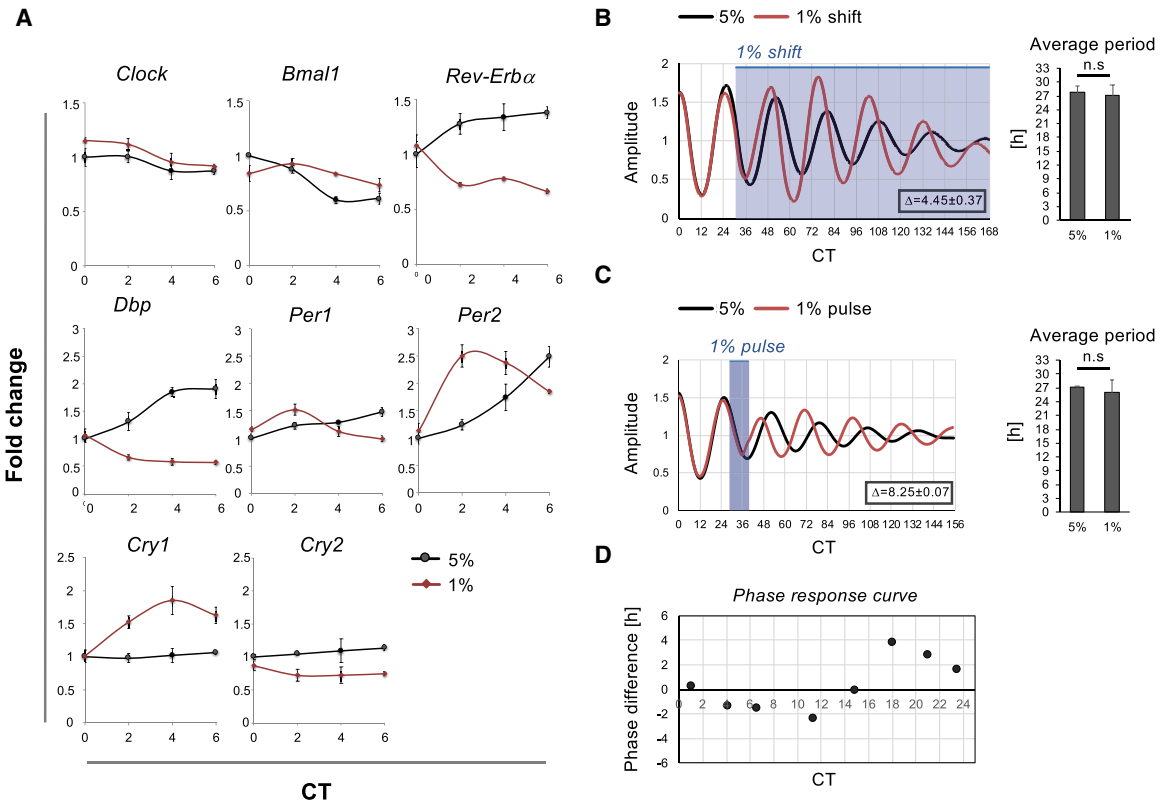

Figure 7. Carbon Dioxide Levels Affect Core Clock Gene Expression and Phase Shift the Clock

(A) NIH3T3 cells were maintained at 5% CO_2. After 3 days in culture, cells were either shifted to 1% CO_2 or kept at 5% CO_2 as control. Cells were harvested at indicated times. Total RNA was prepared and transcript levels of clock genes were determined by quantitative real-time PCR and presented as fold change relative to the lowest value.

(B) Bioluminescence recordings of NIH3T3 stably expressing *Bmal1*-luciferase reporters that were cultured either at 5% CO_2 or shifted to constant 1% CO_2. The alongside bar graph represents the average circadian period ± SEM.

(C) Bioluminescence recordings of NIH3T3 stably expressing *Bmal1*-luciferase reporters that were cultured either at 5% CO_2 or were exposed to a 10 h pulse of 1% CO_2. The alongside bar graph represents the average circadian period ± SEM.

(D) Phase response curve in response to 2 h pulses of 1% CO_2. The x axis indicates the circadian time at the beginning of the pulse. The y axis indicates the phase shift resulted from the pulse. The bioluminescence recordings for each pulse are presented in Figure S5. CT, circadian time; n.s, non-specific.

See also Figure S6.

day and qualifies as type-1 in chronobiological parlance. It is similar to the response observed for light-induced phase shifts of circadian behavior in laboratory animals. Of note, we did not observe any significant effect on the period length in any of the above-described experiments (i.e., 5% to 1% shift, 10 h or 2 h pulse) between the control and the treated cells (Figures 7B, 7C, and S6).

In summary, our results show that changes in carbon dioxide levels are sufficient to affect the expression of several core clock genes and phase shift the clock at least in cultured cells. It is, therefore, possible that the observed change in carbon dioxide rhythmicity upon day-time feeding plays a role in the inversion of circadian clocks in peripheral tissues in this conjuncture.

DISCUSSION

Detailed measurements of behavioral (e.g., activity, feeding) alongside physiological parameters (e.g., respiration) are evidently necessary for uncovering regulatory principles that dictate their daily changes both endogenously and in response to environmental changes (Acosta-Rodríguez et al., 2017). In this conjuncture, there is a growing usage of metabolic cages that continuously monitor oxygen consumption and carbon dioxide release for energy production calculations (i.e., indirect calorimetry) together with activity and food intake to follow daily physiology and behavior (Mina et al., 2018; Tschöp et al., 2011).

In this study, we monitored oxygen consumption, carbon dioxide release, food intake, and spontaneous locomotor activity, alongside tissue oxygenation in freely moving animals to dissect the daily control of oxygen and carbon dioxide rhythms by circadian clocks, light-dark cycles, and feeding cycles. Our analyses of two different circadian clock mutant mouse models (i.e., PER1/2 and BMAL1 null mice) under free running conditions (i.e., constant dark) strongly suggest that circadian clocks control daily rhythms in oxygen and carbon dioxide. It is likely that the effect is indirect and is the consequence of rhythmic activity and feeding behavior that are driven by the circadian clock. Both PER1/2 and BMAL1 null mice exhibited overt rhythms in

respiration when housed under a 12 h light-dark regimen, yet BMAL1-deficient mice showed a shallower amplitude. The BMAL1 null mice were previously shown to exhibit early aging and age-related pathologies (Kondratov et al., 2006); however, in our experiments with ~3-month-old mice, we did not observe any overt signs of aging, and their total oxygen consumption, carbon dioxide release, activity, and feeding were comparable to the wild-type control group. It is possible that the abrogated circadian amplitude in the aforementioned parameters precedes and even plays a role in the accelerated aging phenotype of these mice.

Intriguingly, the clock mutant CRY1/2 null mice were reported to show no rhythmicity in their respiratory exchange rate (RER) (i.e., the ratio between carbon dioxide release and oxygen consumption) under the light-dark regimen (Vollmers et al., 2009). It is unclear whether the observed difference between CRY1/2 and the PER1/2-deficient and BMAL1-deficient mice in our experiments reflects a true biological effect, or rather stems from technical factors (e.g., light intensity and/or spectrum and statistical analysis). Of note, the statistical toolkit for circadian analyses mostly relies on fitting a cosine curve and hence is not ideal for analysis of the square-shaped rhythms that are often observed for oxygen consumption, carbon dioxide release, activity, and food intake. Future studies are expected to clarify whether CRY1/2-deficient mice indeed differ from BMAL1 and PER1/2 null mice in regard to their rhythmic respiration under light-dark cycles.

Our experiments evinced that both light-dark cycles and feeding-fasting rhythms are sufficient and as effective in driving rhythmicity in oxygen consumption and carbon dioxide release with comparable phases and amplitudes in the absence of a functional clock (i.e., BMAL1 and PER1/2 null mice). Similar effect of feeding-fasting cycles was observed with CRY1/2-deficient animals (Vollmers et al., 2009). Notably, mice that are on a high-fat diet lose their rhythmic feeding behavior and exhibit altered circadian gene expression (Eckel-Mahan et al., 2013; Hatori et al., 2012; Kohsaka et al., 2007). Upon this nutritional challenge, time-restricted feeding restores rhythms in RER and oxygen consumption as well independently of the circadian clock (Chaix et al., 2018). It, therefore, appears that light-dark cycles can drive rhythmic feeding behavior, which in turn generates rhythms in oxygen and carbon dioxide independently of the clock. Another nutritional challenge that was recently shown to alter circadian gene expression is ketogenic diet (Tognini et al., 2017). Interestingly, a ketogenic diet, similar to the high-fat diet, diminishes daily RER rhythmicity; however, it does not affect the animals' rhythmic feeding behavior. Overall, these studies highlight the importance of the diet composition on daily respiration.

Consistent with our model that carbon dioxide oscillations are directed by feeding, we noted a trend of higher amplitude in carbon dioxide oscillations upon feeding rhythms compared to light-dark cycles and a sharp decline over 24 h of food deprivation. Furthermore, day-time feeding dissociated oxygen rhythms from carbon dioxide oscillations, whereby the former followed activity and the latter was shifted and aligned with food intake. The bimodal profile of oxygen and activity and the inversion in carbon dioxide were independent of light-dark cycles and the circadian clock. Thus, they appear as a direct response to food intake. It is plausible that the sharp spike in oxygen and activity at the dark-light transition upon day-time feeding most likely reflects the sharp bout of activity and food consumption right at the start of the unexpected food availability.

In the above-described experiments, both mice and rats were housed in standard animal facilities with ambient temperature of ~22°C. This was set primarily to match the comfort requirement of the experimenters and the animal facility staff but is far from the thermoneutral temperature of rodents, which is ~30°C. Consequently, rodents increase their energy expenditure in order to maintain their homeothermy, and as a result, the observed oxygen consumption levels are higher than expected for a typical mammal of their size (Schmidt-Nielsen, 1983). Despite the non-thermoneutral conditions and in agreement with the works of others and our own, mice show a clear diurnal pattern of energy expenditure, with night-time levels being higher than day-time (Fischer et al., 2018). Hence, although there is an ongoing debate concerning optimal housing temperatures for mice to better model human metabolism and disease (Gaskill and Garner, 2014; Karp, 2012; Speakman and Keijer, 2012) the non-thermoneutral conditions that were maintained throughout this entire study are widely common and most likely did not affect the presence of daily rhythms. It is noteworthy that since oxygen consumption in mammals per unit body mass decreases regularly with increasing body size (Schmidt-Nielsen, 1983), it explains the difference in the magnitude of oxygen consumption between male and female mice (females are smaller than males), as well as between mice and rats (the latter are bigger).

While the master clock in the SCN region of the brain is entrained by light-dark cycles, feeding rhythms serve as the dominant timing cue for peripheral clocks (Dibner et al., 2010). The adaptation of peripheral clocks to changes in feeding regimen (e.g., from night-fed to day-fed) is gradual and normally takes several days. The process most likely involves a wide variety of signaling pathways that work in concert. Therefore, kinetic experiments turned out to be instrumental in addressing potential mechanisms that are implicated in the processes (Asher and Schibler, 2011). The immediate and sustained response of respiration to changes in feeding regimen hinted at the potential involvement of blood gases in phase resetting of peripheral clocks. Recently we showed that oxygen can reset peripheral clocks through HIF1α (Adamovich et al., 2017). Here, we examined the potential of carbon dioxide to phase shift the clocks. At least in cultured cells, carbon dioxide levels altered core clock gene expression and induced a prominent phase shift, thus supporting a potential role for carbon dioxide in phase resetting of circadian clocks in peripheral organs *in vivo*. Since carbon dioxide levels play a major role in acid-base balance, it is possible that the effect of carbon dioxide on the clock is mediated via changes in pH levels. Indeed, it was previously reported that pH levels can phase shift the clock (Kon et al., 2008). Interestingly, cells can sense changes in carbon dioxide levels irrespectively of changes in pH (Cummins et al., 2014), this raises the intriguing possibility that similar to carbon monoxide (Dioum et al., 2002; Klemz et al., 2017), carbon dioxide directly and independently of pH affects the clocks. Future studies are expected to shed light on the potential molecular mechanism implicated in the effect of carbon dioxide on the core clock circuitry and its interplay with other resetting cues such as oxygen and temperature. These mechanisms are probably not mutually exclusive and might very well act together to phase shift clocks in peripheral organs.

Overall, the current study dissects the function of circadian clocks, light-dark and feeding cycles in control of oxygen and carbon dioxide rhythms and supports a potential role for carbon dioxide in phase resetting of peripheral clocks. Our findings that day-time feeding dissociate oxygen rhythms from carbon dioxide oscillations are potentially of clinical relevance. For example, feeding-activity misalignment results in oxygen-carbon dioxide mismatch and likely affects acid-base balance. These homeostatic imbalances potentially play a role in pathologies associated with altered feeding-activity rhythms, for example, in shift-workers (Brum et al., 2015).

Limitations of the Study

Our study mostly relies on metabolic cage measurements of oxygen consumption, carbon dioxide release, activity, and feeding behavior and on alongside telemetric measurements of tissue oxygenation in freely moving animals. However, the latter, as above mentioned, are limited to rats, and currently because of technical limitations cannot be performed with mice (of particular interest are the different clock mutant mouse models). Moreover, telemetric measurements of a tissues' carbon dioxide levels in freely moving animals are currently technically unfeasible. We show that oxygen and carbon dioxide rhythms are circadian clock controlled, most likely indirectly through rhythmic activity and feeding behavior that are driven by the clock. Yet, we cannot exclude the possibility that peripheral clocks in various tissues are directly implicated as well. Lastly, we provide evidence that oxygen rhythms are dominated by activity while carbon dioxide oscillations align with food intake. It is practically impossible to completely uncouple activity from feeding, likewise oxygen consumption from carbon dioxide release. Hence, at this stage, we can only point toward the dominance of activity on oxygen consumption and food intake on carbon dioxide release.

STAR★METHODS

Detailed methods are provided in the online version of this paper and include the following:

- KEY RESOURCES TABLE
- CONTACT FOR REAGENT AND RESOURCE SHARING
- EXPERIMENTAL MODEL DETAILS
  - Animals
- METHOD DETAILS
  - Metabolic Cages
  - Time-Restricted Feeding
  - Tissue Oxygenation Measurement
  - Cell Lines
  - Real-Time Bioluminescence Monitoring
  - Gene Expression Analysis
- QUANTIFICATION AND STATISTICAL ANALYSIS
  - Cosine Fits
  - Peak Detection
  - Statistical Analysis

SUPPLEMENTAL INFORMATION

Supplemental Information includes six figures and one table and can be found with this article online at https://doi.org/10.1016/j.cmet.2019.01.007.

ACKNOWLEDGMENTS

We are grateful to the members of the Asher lab for their valuable comments on the manuscript. We thank Sharon Ovadia and Beni Sioani for their assistance with the animal care and Asher Auerbach for his technical assistance. G.A. is supported by the European Research Council (ERC-2017 CIRCOMMUNICATION 770869) and is recipient of the EMBO young investigator award. Work in M.K. laboratory was supported by the British Heart Foundation (No. FS/14/2/30630) and the European Union, Seventh Framework Program, Marie Curie Actions (CARPEDIEM – No. 612280). Y.K. is the incumbent of the Sarah and Rolandu Uziel Research Associate Chair. J.S. is recipient of a fellowship from the Placid Nicod foundation.

AUTHOR CONTRIBUTIONS

Conceptualization, Y.A., B.L., and G.A; Investigation, Y.A., B.L., A.N.-C., M.G., Y.K., M.H.A., A.T., and M.P.K; Visualization, Y.A., B.L., and J.S.; Data Curation, J.S.; Software, J.S.; Funding, G.A.; Writing – Review & Editing, Y.A., B.L., and G.A.

DECLARATION OF INTERESTS

The authors declare no competing interests.

Received: December 4, 2017
Revised: November 13, 2018
Accepted: January 16, 2019
Published: February 14, 2019

REFERENCES

Acosta-Rodríguez, V.A., de Groot, M.H.M., Rijo-Ferreira, F., Green, C.B., and Takahashi, J.S. (2017). Mice under caloric restriction self-impose a temporal restriction of food intake as revealed by an automated feeder system. Cell Metab. *26*, 267–277.

Adamovich, Y., Ladeuix, B., Golik, M., Koeners, M.P., and Asher, G. (2017). Rhythmic oxygen levels reset circadian clocks through HIF1alpha. Cell Metab. *25*, 93–101.

Adamovich, Y., Rousso-Noori, L., Zwighaft, Z., Neufeld-Cohen, A., Golik, M., Kraut-Cohen, J., Wang, M., Han, X., and Asher, G. (2014). Circadian clocks and feeding time regulate the oscillations and levels of hepatic triglycerides. Cell Metab. *19*, 319–330.

Akram, M. (2014). Citric acid cycle and role of its intermediates in metabolism. Cell Biochem. Biophys. *68*, 475–478.

Asher, G., Reinke, H., Altmeyer, M., Gutierrez-Arcelus, M., Hottiger, M.O., and Schibler, U. (2010). Poly(ADP-ribose) polymerase 1 participates in the phase entrainment of circadian clocks to feeding. Cell *142*, 943–953.

Asher, G., and Sassone-Corsi, P. (2015). Time for food: the intimate interplay between nutrition, metabolism, and the circadian clock. Cell *161*, 84–92.

Asher, G., and Schibler, U. (2011). Crosstalk between components of circadian and metabolic cycles in mammals. Cell Metab. *13*, 125–137.

Bass, J., and Lazar, M.A. (2016). Circadian time signatures of fitness and disease. Science *354*, 994–999.

Brum, M.C., Filho, F.F., Schnorr, C.C., Bottega, G.B., and Rodrigues, T.C. (2015). Shift work and its association with metabolic disorders. Diabetol. Metab. Syndr. *7*, 45.

Bunger, M.K., Wilsbacher, L.D., Moran, S.M., Clendenin, C., Radcliffe, L.A., Hogenesch, J.B., Simon, M.C., Takahashi, J.S., and Bradfield, C.A. (2000). Mop3 is an essential component of the master circadian pacemaker in mammals. Cell *103*, 1009–1017.

Chaix, A., Lin, T., Le, H.D., Chang, M.W., and Panda, S. (2018). Time-restricted feeding prevents obesity and metabolic syndrome in mice lacking a circadian clock. Cell Metab. *18*, 30505–30509.

Cornelissen, G. (2014). Cosinor-based rhythmometry. Theor. Biol. Med. Model. *11*, 16.

Cummins, E.P., Selfridge, A.C., Sporn, P.H., Sznajder, J.I., and Taylor, C.T. (2014). Carbon dioxide-sensing in organisms and its implications for human disease. Cell. Mol. Life Sci. *71*, 831–845.

Curtis, A.M., and Fitzgerald, G.A. (2006). Central and peripheral clocks in cardiovascular and metabolic function. Ann. Med *38*, 552–559.

Damiola, F., Le Minh, N., Preitner, N., Kornmann, B., Fleury-Olela, F., and Schibler, U. (2000). Restricted feeding uncouples circadian oscillators in peripheral tissues from the central pacemaker in the suprachiasmatic nucleus. Genes Dev. *14*, 2950–2961.

Dibner, C., Schibler, U., and Albrecht, U. (2010). The mammalian circadian timing system: organization and coordination of central and peripheral clocks. Annu. Rev. Physiol. *72*, 517–549.

Dioum, E.M., Rutter, J., Tuckerman, J.R., Gonzalez, G., Gilles-Gonzalez, M.A., and McKnight, S.L. (2002). NPAS2: a gas-responsive transcription factor. Science *298*, 2385–2387.

Eckel-Mahan, K.L., Patel, V.R., de Mateo, S., Orozco-Solis, R., Ceglia, N.J., Sahar, S., Dilag-Penilla, S.A., Dyar, K.A., Baldi, P., and Sassone-Corsi, P. (2013). Reprogramming of the circadian clock by nutritional challenge. Cell *155*, 1464–1478.

Emans, T.W., Janssen, B.J., Joles, J.A., and Krediet, C.T.P. (2017). Circadian rhythm in kidney tissue oxygenation in the rat. Front. Physiol. *8*, 205.

Fischer, A.W., Cannon, B., and Nedergaard, J. (2018). Optimal housing temperatures for mice to mimic the thermal environment of humans: an experimental study. Mol. Metab. *7*, 161–170.

Gaskill, B.N., and Garner, J.P. (2014). Letter-to-the-editor on "Not so hot: optimal housing temperatures for mice to mimic the thermal environment of humans". Mol. Metab. *3*, 335–336.

Hatori, M., Vollmers, C., Zarrinpar, A., DiTacchio, L., Bushong, E.A., Gill, S., Leblanc, M., Chaix, A., Joens, M., Fitzpatrick, J.A., et al. (2012). Time-restricted feeding without reducing caloric intake prevents metabolic diseases in mice fed a high-fat diet. Cell Metab. *15*, 848–860.

Hogenesch, J.B., Gu, Y.Z., Jain, S., and Bradfield, C.A. (1998). The basic-helix-loop-helix-PAS orphan MOP3 forms transcriptionally active complexes with circadian and hypoxia factors. Proc. Natl. Acad. Sci. U S A *95*, 5474–5479.

Karp, C.L. (2012). Unstressing intemperate models: how cold stress undermines mouse modeling. J. Exp. Med. *209*, 1069–1074.

Klemz, R., Reischl, S., Wallach, T., Witte, N., Jürchott, K., Klemz, S., Lang, V., Lorenzen, S., Knauer, M., Heidenreich, S., et al. (2017). Reciprocal regulation of carbon monoxide metabolism and the circadian clock. Nat. Struct. Mol. Biol. *24*, 15–22.

Koeners, M.P., Ow, C.P., Russell, D.M., Abdelkader, A., Eppel, G.A., Ludbrook, J., Malpas, S.C., and Evans, R.G. (2013). Telemetry-based oxygen sensor for continuous monitoring of kidney oxygenation in conscious rats. Am. J. Physiol. Renal Physiol. *304*, F1471–F1480.

Koeners, M.P., Ow, C.P.C., Russell, D.M., Evans, R.G., and Malpas, S.C. (2016). Prolonged and continuous measurement of kidney oxygenation in conscious rats. Methods Mol. Biol. *1397*, 93–111.

Kohsaka, A., Laposky, A.D., Ramsey, K.M., Estrada, C., Joshu, C., Kobayashi, Y., Turek, F.W., and Bass, J. (2007). High-fat diet disrupts behavioral and molecular circadian rhythms in mice. Cell Metab. *6*, 414–421.

Kon, N., Hirota, T., Kawamoto, T., Kato, Y., Tsubota, T., and Fukada, Y. (2008). Activation of TGF-beta/activin signalling resets the circadian clock through rapid induction of Dec1 transcripts. Nat. Cell Biol. *10*, 1463–1469.

Kondratov, R.V., Kondratova, A.A., Gorbacheva, V.Y., Vykhovanets, O.V., and Antoch, M.P. (2006). Early aging and age-related pathologies in mice deficient in BMAL1, the core componentof the circadian clock. Genes Dev. *20*, 1868–1873.

Manella, G., and Asher, G. (2016). The circadian nature of mitochondrial biology. Front. Endocrinol. (Lausanne) *7*, 162.

Meyer, C.W., Reitmeir, P., and Tschöp, M.H. (2015). Exploration of energy metabolism in the mouse using indirect calorimetry: measurement of daily energy expenditure (DEE) and basal metabolic rate (BMR). Curr. Protoc. Mouse Biol. *5*, 205–222.

Mina, A.I., LeClair, R.A., LeClair, K.B., Cohen, D.E., Lantier, L., and Banks, A.S. (2018). CalR: A web-based analysis tool for indirect calorimetry experiments. Cell Metab. *28*, 656–666.

Mortola, J.P. (2004). Breathing around the clock: an overview of the circadian pattern of respiration. Eur. J. Appl. Physiol. *91*, 119–129.

Mukherji, A., Kobiita, A., and Chambon, P. (2015). Shifting the feeding of mice to the rest phase creates metabolic alterations, which, on their own, shift the peripheral circadian clocks by 12 hours. Proc. Natl. Acad. Sci. U S A *112*, E6683–E6690.

Nagoshi, E., Saini, C., Bauer, C., Laroche, T., Naef, F., and Schibler, U. (2004). Circadian gene expression in individual fibroblasts: cell-autonomous and self-sustained oscillators pass time to daughter cells. Cell *119*, 693–705.

Neufeld-Cohen, A., Robles, M.S., Aviram, R., Manella, G., Adamovich, Y., Ladeuix, B., Nir, D., Rousso-Noori, L., Kuperman, Y., Golik, M., et al. (2016). Circadian control of oscillations in mitochondrial rate-limiting enzymes and nutrient utilization by PERIOD proteins. Proc. Natl. Acad. Sci. U S A *113*, E1673–E1682.

Panda, S. (2016). Circadian physiology of metabolism. Science *354*, 1008–1015.

Partch, C.L., Green, C.B., and Takahashi, J.S. (2014). Molecular architecture of the mammalian circadian clock. Trends Cell Biol. *24*, 90–99.

Peek, C.B., Affinati, A.H., Ramsey, K.M., Kuo, H.Y., Yu, W., Sena, L.A., Ilkayeva, O., Marcheva, B., Kobayashi, Y., Omura, C., et al. (2013). Circadian clock NAD^+ cycle drives mitochondrial oxidative metabolism in mice. Science *342*, 1243417.

Peek, C.B., Levine, D.C., Cedernaes, J., Taguchi, A., Kobayashi, Y., Tsai, S.J., Bonar, N.A., McNulty, M.R., Ramsey, K.M., and Bass, J. (2017). Circadian clock interaction with HIF1alpha mediates oxygenic metabolism and anaerobic glycolysis in skeletal muscle. Cell Metab. *25*, 86–92.

Saini, C., Liani, A., Curie, T., Gos, P., Kreppel, F., Emmenegger, Y., Bonacina, L., Wolf, J.P., Poget, Y.A., Franken, P., et al. (2013). Real-time recording of circadian liver gene expression in freely moving mice reveals the phase-setting behavior of hepatocyte clocks. Genes Dev. *27*, 1526–1536.

Schmidt-Nielsen, K. (1983). Animal Physiology: Adaptation and Environment/ Knut Schmidt-Nielsen (Cambridge University Press).

Sobel, J.A., Krier, I., Andersin, T., Raghav, S., Canella, D., Gilardi, F., Kalantzi, A.S., Rey, G., Weger, B., Gachon, F., et al. (2017). Transcriptional regulatory logic of the diurnal cycle in the mouse liver. PLoS Biol. *15*, e2001069.

Speakman, J.R., and Keijer, J. (2012). Not so hot: optimal housing temperatures for mice to mimic the thermal environment of humans. Mol. Metab. *2*, 5–9.

Stokkan, K.A., Yamazaki, S., Tei, H., Sakaki, Y., and Menaker, M. (2001). Entrainment of the circadian clock in the liver by feeding. Science *291*, 490–493.

Takahashi, J.S. (2017). Transcriptional architecture of the mammalian circadian clock. Nat. Rev. Genet. *18*, 164–179.

Tognini, P., Murakami, M., Liu, Y., Eckel-Mahan, K.L., Newman, J.C., Verdin, E., Baldi, P., and Sassone-Corsi, P. (2017). Distinct circadian signatures in liver and gut clocks revealed by ketogenic diet. Cell Metab. *26*, 523–538.

Tschöp, M.H., Speakman, J.R., Arch, J.R., Auwerx, J., Brüning, J.C., Chan, L., Eckel, R.H., Farese, R.V., Jr., Galgani, J.E., Hambly, C., et al. (2011). A guide to analysis of mouse energy metabolism. Nat. Methods *9*, 57–63.

Vollmers, C., Gill, S., DiTacchio, L., Pulivarthy, S.R., Le, H.D., and Panda, S. (2009). Time of feeding and the intrinsic circadian clock drive rhythms in hepatic gene expression. Proc. Natl. Acad. Sci. U S A *106*, 21453–21458.

Wilson, D.F., Rumsey, W.L., Green, T.J., and Vanderkooi, J.M. (1988). The oxygen dependence of mitochondrial oxidative phosphorylation measured by a new optical method for measuring oxygen concentration. J. Biol. Chem. *263*, 2712–2718.

Wu, Y., Tang, D., Liu, N., Xiong, W., Huang, H., Li, Y., Ma, Z., Zhao, H., Chen, P., Qi, X., et al. (2017). Reciprocal regulation between the circadian clock and hypoxia signaling at the genome level in mammals. Cell Metab. *25*, 73–85.

Zheng, B., Albrecht, U., Kaasik, K., Sage, M., Lu, W., Vaishnav, S., Li, Q., Sun, Z.S., Eichele, G., Bradley, A., et al. (2001). Nonredundant roles of the mPer1 and mPer2 genes in the mammalian circadian clock. Cell *105*, 683–694.

STAR★METHODS

KEY RESOURCES TABLE

REAGENT or RESOURCE	SOURCE	IDENTIFIER
Chemicals, Peptides, and Recombinant Proteins		
Ortho-phthalaldehyde	Cidex OPA	
Buprenorphine	Temgesic, Reckitt Benckiser, Slough, UK	
Sodium pentobarbitone	Euthatal, Merial, Pirbright, UK	
TRI reagent	Sigma-Aldrich	93289
LightCycler 480 Syber Green I Master	Roche	04 707 516 001
LightCycler 480 Probe Master	Roche	04 707 494 001
Luciferin	Promega	E1601
Critical Commercial Assays		
qScript cDNA synthesis kit	Quantabio	95047
Experimental Models: Organisms/Strains		
Mouse: wild-type C57BL/6	Envigo	
Mouse: *Bmal1*$^{-/-}$ C57BL/6 A.K.A *Arntl*^{tm1Bra}	Jackson Laboratory (Bunger et al., 2000)	
Mouse: *Per1/2*$^{-/-}$ C57BL/6	(Zheng et al., 2001)	
Rat: Wistar	Harlan	
Experimental Models: Cell Lines		
NIH 3T3 *Bmal*-luciferase	(Nagoshi et al., 2004)	
Oligonucleotides		
Primers and probes for real-time PCR are listed in Table S1	Supplemental data in the current paper	
Software and Algorithms		
R	CRAN	v 3.5.0
dplyr	CRAN	v 0.7.7
ggplot2	CRAN	v 3.0.0
zoo	CRAN	v 1.8-4
MATLAB	MathWorks	R2017b
MetaScreen, used for data collection	Sable Systems International, Las Vegas, NV,USA.	v 2.3.14.6
ExpeData, used for data analysis	Sable Systems International, Las Vegas, NV,USA.	v 1.9.14
LumiCycle analysis software	Actimetrics	
Other		
Regular chow	Envigo	2018 Teklad
Rodent diet	Ssniff Spezialdiaten GmbH	V1154-703
Phenomaster metabolic cages	TSE Systems	
Promethion indirect calorimeter system	Sable Systems International, las vegas, NV, USA	
Oxygen telemeter	Millar Inc., Houston, TX, USA	TR57Y
SmartPad	Millar Inc., Houston, TX, USA	TR181
Tissue glue	Histoacryl, Braun, Tuttlingen, Germany	1050044 B
LumiCycle	Actimetrics	

CONTACT FOR REAGENT AND RESOURCE SHARING

Further information and requests for resources and reagents should be directed to and will be fulfilled by the Lead Contact, Gad Asher (gad.asher@weizmann.ac.il).

EXPERIMENTAL MODEL DETAILS

Animals

All animal experiments and procedures were conducted in conformity with the Weizmann Institute Institutional Animal Care and Use Committee guidelines, the Ben-Gurion University of the Negev Animal Use and Care Committee protocol number: IL-77-11-2015 and the UK Home Office (Scientific Procedures) Act (1986) with project approval from the ethics of research committee, University of Bristol. For metabolic cages analyses, we used three months old Wistar rats and C57BL/6 wild type, *Per1/2*$^{-/-}$ (Zheng et al., 2001) back crossed to C57BL/6 and C57BL/6 *Bmal1*$^{-/-}$ (Bunger et al., 2000) mice. For telemetric oxygen monitoring three months old Wistar rats were used. Animals were housed under 12 h light-dark regimen or constant dark and fed either *ad libitum* or exclusively during the dark or light phase as indicated. The temperature in the housing cages and metabolic cages was maintained at 22°C. ZT0 corresponds to the time lights were turned ON and ZT12 to the time lights were turned OFF in the animal facility.

METHOD DETAILS

Metabolic Cages

Mice and rats' oxygen consumption rate, carbon dioxide release, spontaneous locomotor activity and food consumption were simultaneously monitored for individually housed mice using the Phenomaster metabolic cages (TSE System) and Promethion metabolic cages (Sable Systems International), respectively. Before each experiment animals were trained for several days in the metabolic cages to enable them to properly adjust to the new housing conditions. A period of 3-7 days acclimatization was taken before the actual recordings. Data was collected at 15 min intervals for TSE, and 1 min for Sable system. All animals presented per figure were recorded together side by side to allow adequate comparisons. The light schedule in the metabolic cages was maintained as in the animals' home cages. Fluorescent light with intensity of 100 lux was applied for the metabolic cage recordings during the light phase.

Time-Restricted Feeding

The same cohort of animals was fed according to the different feeding schedule per figure as indicated in the figure legend. Transition from *ad libitum* to night-time feeding was done with a 12 h fasting period during the light phase, and from night to day-time feeding with a 24 h fasting period. Time-restricted feeding was performed either manually (rats), or using automated feeders (mice).

Tissue Oxygenation Measurement

Oxygen levels in rat kidney/liver were measured using a telemetry system as described previously (Koeners et al., 2013, 2016). Telemeters (TR57Y) equipped with a carbon paste electrode (CPE, 0.27 mm in diameter) were sterilized in a 2% w/v glutaraldehyde solution for at least 4 hours or 0.55% w/v ortho-phthalaldehyde (Cidex OPA) for 30 minutes and rinsed thoroughly with sterile 0.9% w/v NaCl solution before implantation. Rats were anaesthetized with 5% v/v isofluorane in an induction box and maintained at 2–2.5 % v/v isoflurane on a heated operating table. Rats were pre-medicated with buprenorphine (30 μg/kg s.c., Temgesic, Reckitt Benckiser, Slough, UK). Under sterile conditions, the kidney/liver and aorta were exposed by laparotomy. The cables connecting the electrodes and telemeter were secured by suturing them on the adventitia of the abdominal aorta or dorsal muscles adjacent to the spine near the kidney/liver. After pre-puncturing the tissue with a 30-gauge needle, the reference electrode and CPE, were inserted and secured in place with tissue glue (Histoacryl, 1050044 B. Braun, Tuttlingen, Germany) approximately 1 mm apart from each other, while the auxiliary electrode was affixed onto the tissue surface. With the telemeter placed and secured in the abdomen, the abdomen was closed with sutures and the rat was placed on a heated pad for at least 12 hours to recover. Post-operative analgesia was administered (buprenorphine, 3 μg/100 g rat every 8–14 h for up to 3 days or as required). All rats were allowed to recover for 1 week before experiments started. After a recovery, the rat's cage was placed on a receiver-charging unit (SmartPad TR181, Millar Inc, Tx), which received the data from, and recharged the battery of, the telemeter. Renal/hepatic O_2 levels were continuously measured in Wistar rats for several consecutive days. After the experimental period, rats were sacrificed by intraperitoneal injection of an overdose of sodium pentobarbitone (>200 mg ml-1, Euthatal, Merial, Pirbright, UK) and post-mortem O_2 values were determined for off-set correction of individual O_2 recordings

Cell Lines

A stable NIH 3T3 cell line expressing *Bmal1*-luciferase (Nagoshi et al., 2004) was cultured in DMEM containing 10% FBS, 100IU/ml penicillin and 100mg/ml streptomycin at 37°C in a humidified incubator with 5% CO_2 unless indicated otherwise.

Real-Time Bioluminescence Monitoring

Cells ($0.2x10^6$ cells/plate) were seeded in 35mm culture dishes and cultured for 2 days. Cell culture media was replaced to DMEM without phenol red supplemented with luciferine and cells were placed in the LumiCycle for continuous bioluminescence recordings for several consecutive days. CO_2 levels were either kept at 5% (control) or reduced to 1% for periods indicated in the main text and figure legends. Data was analyzed with the LumiCycle analysis software (Actimetrics).

Gene Expression Analysis

Total RNA was extracted from mouse liver tissue using TRI reagent (Sigma Aldrich). RNA quality and quantity were measured using Nanodrop (Thermo Scientific). cDNA synthesis was performed using qScript (Quantabio). RNA expression analysis was performed by real-time PCR using SYBR green or Taqman probes with LightCycler II machine (Roche). Expression levels were calculated using the ΔΔcT method and normalized to the geometrical mean of three housekeeping genes: *Hprt*, *Rplp0*, *Tbp*. Primers and probes (Sigma) are listed in Table S1.

QUANTIFICATION AND STATISTICAL ANALYSIS

Cosine Fits

Rhythmicity analysis was done as previously described (Sobel et al., 2017) using harmonic regression. Briefly, we used the function $x(t) = A_0 + A_{24}\cos(2\pi/(24\ \text{h}) * (t - t_{max}))$, where A_0 is the mean signal, A_{24} the amplitude of the 24h oscillations, and t_{max} the phase (or peak time). This method is also known as the single Cosinor model (Cornelissen, 2014). Thus, using this model, we performed least squared fitting of activity, feeding, VO_2 and VCO_2 data in each experimental condition. The following exclusion criteria was used: the cosine fit, although having a significant p-value, was considered as biologically non-relevant in case the amplitude divided by the S.D. of the data was below 1 (marked with # in the relevant figures).

Peak Detection

Peak detection was performed using the built-in function findpeaks() in MATLAB, on smoothed data of 1.75 h running-average window. The function parameter values that were used: minimal peak prominence of 2 standard deviations of the signal, minimal peak distance of 6 h, and minimal peak height defined as the signal mean level.

Statistical Analysis

Details regarding sample size and statistical tests are indicted in the figure legends. A two-tail Student's t tests unpaired (for amplitude and total per day) or paired (for Light phase vs Dark phase) were used with * for $p < 0.05$, ** for $p < 0.01$ and *** for $p < 0.001$. Data visualizations are depicted with the average of biological replicates ± standard error of the mean. Statistical significance was concluded at $p < 0.05$. Telemetric data are represented with a 3 h smoothing window overlapped with the raw data (every minute). Statistics were calculated with R and Excel statistical features.